Journal of Organometallic Chemistry 896 (2019) 70–76

Contents lists available at ScienceDirect

Journal of Organometallic Chemistry

journal homepage: www.elsevier.com/locate/jorganchem

Unusual resistance of cobalt bis dicarbollide phosphate and phosphorothioate bridged esters towards alkaline hydrolysis: The "metallacarborane effect"

Carla Sardo, Sławomir Janczak, Zbigniew J. Leśnikowski*

Laboratory of Medicinal Chemistry, Institute of Medical Biology PAS, Lodowa 106, 93-232, Lodz, Poland

ARTICLE INFO

Article history:
Received 12 April 2019
Received in revised form
23 May 2019
Accepted 3 June 2019
Available online 5 June 2019

Keywords:
Cobalt bis dicarbollide
Phosphate
Phosphorothioate
Bridged metallacarborane
Hydrolysis

ABSTRACT

The extraordinary stability of bridged O,O-[cobalt bis(dicarbollide)ion] O-(4-nitrophenyl)phosphorothioate **[2]**$^-$ and phosphate **[3]**$^-$ esters under alkali conditions was discovered. The hydrolysis of metallacarborane esters **[2]**$^-$ and **[3]**$^-$ was studied, and the kinetic and thermodynamic parameters were measured and compared with those of their organic counterparts, parathion and paraoxon. The extreme differences between the hydrolytic properties of alkyl- and metallacarborane phosphate and phosphorothioate esters are attributed to the electronic and steric effects of the metallacarborane non leaving group ("metallacarborane effect"). The known "thio effect" contributes to a lesser extent to the resistance of **[2]**$^-$ to the basic conditions.

1. Introduction

One of the important features of polyhedral boron clusters [1–3] is the ability to coordinate a broad range of metal ions such as Fe, Co, Cr, Ta, Mo, W, V, Nb, forming coordination compounds, that is, metallacarboranes [4–7]. Since the discovery of icosahedral metallacarboranes [3,3′-M(1,2-$C_2B_9H_{11}$)$_2$]$^-$, one of the subsets of this class of metal complexes half a century ago by M.F. Hawthorne [8], they have been a subject of ongoing interest. The reasons for this are unique features of metallacrboranes such as rigid cage, rotary motion, hydrophobicity or amphiphilicity, redox activity and remarkable chemical and thermal stability of the caged core structure [9]. Among them, a widely employed metallacarborane is a sandwich of two [$C_2B_9H_{11}$]$^{2-}$ (dicarbollide) clusters with a cobalt ion in the center of the complex structure [10]. Derivatives of cobalt(III) bis(1,2-dicarbollide) anion have applications in different areas such as remediation of nuclear wastes [11,12], radio-imaging and medicinal chemistry [13].

One of the exciting applications of metallacarboranes is as catalysts. The use of metallacarboranes as catalytic system for different reactions is underrated but the potential has been demonstrated more than once. For example, the usefulness of Li[3,3′-Co(1,2-$C_2B_9H_{11}$)$_2$] as Lewis acid in the catalysis of the addition of silyl ketene acetals to hindered α,β-unsaturated carbonyl compounds [14] and for the substitution of allylic acetates with various nucleophiles [15] was reported. More recently, we have shown that phosphoric acid bridged 8,8′-dihydroxy-cobalt bis(dicarbollide) ion is an effective catalyst for the reduction of aryl substituted ketimines to the corresponding secondary amines [16]. In order to explore further modification to improve activity of this promising catalyst, we designed a thiophosphoric analogue intended to be obtained from the hydrolysis of the corresponding phosphorothioate bridged aryl-ester ([8,8′-μ-O_2P(S)O$C_6H_4NO_2$-3,3′-Co(1,2-$C_2B_9H_{10}$)$_2$]$^-$). The extraordinary hydrolytic stability of this aryl phosphorothioate bridged metallacarborane and its phosphate counterpart under extreme conditions (2 M NaOH, elevated temperature) inspired us to study this phenomenon in more detail.

2. Results and discussion

The tendency of cobalt(III) bis(1,2-dicarbollide) anion to form bridged compounds between boron atoms at position 8 and 8′ of the two dicarbollide moieties is well known [17–21]. Bridged thiophosphate [8,8′-μ-O_2P(S)O$C_6H_4NO_2$-3,3′-Co(1,2-$C_2B_9H_{10}$)$_2$]$^-$ **[2]**$^-$ and its oxo-analogue [8,8′-μ-O_2P(O)O$C_6H_4NO_2$-3,3′-Co(1,2-

* Corresponding author.
E-mail address: zlesnikowski@cbm.pan.pl (Z.J. Leśnikowski).

https://doi.org/10.1016/j.jorganchem.2019.06.001
0022-328X/

$C_2B_9H_{10})_2]^-$ **[3]**$^-$ were conveniently prepared by the treatment of 8,8′-bis-hydroxy metallacarborane [8,8′-μ–$(OH)_2$–3,3′-Co(1,2-$C_2B_9H_{10})_2]^-$ with 1 equivalent of the corresponding dichloride ester in pyridine at room temperature (Scheme 1).

The reaction to obtain oxo derivative **[3]**$^-$ is relatively fast (reaching completion after 3 h), while the reaction to obtain **[2]**$^-$ under the same conditions took 24 h. Products **[2]**$^-$ and **[3]**$^-$ were isolated as the triethylammonium salts.

For both the bridged compounds **HNEt$_3$[2]** and **HNEt$_3$[3]** ^{11}B NMR is characterized by a pattern of signals 2:2:4:4:4:2. The first signal at around 23 ppm for both compounds is a singlet integrating for two boron atoms, reasonably 8 and 8′, which is maintained in both proton coupled and decoupled ^{11}B NMR spectra. The spectral pattern reflects an higher symmetry than that expected for a bridged chiral compound [22], resembling that of NMR equivalence of both dicarbollide parts. There is no doubt that **[1]**$^-$ and **[2]**$^-$ are asymmetric chiral anions, considering that the bridging moiety tends to preserve its tetrahedral arrangement around phosphorus. This in turn led to: 1) twisted conformation of carborane ligands around the central cobalt atom; 2) inclination of P = X bond (X: O or S) toward one carborane ligand and $POPhNO_2$ bond toward the other side of the molecule. Also the non-perfectly parallel pentagonal faces connected with the cobalt atom (behavior that is typical of bridged dicarbollide ligands) contribute to the overall asymmetry of this compounds. Moreover, in a past study involving similar compounds [23], Plešek and colleagues were able to determine the absolute configuration of one enantiomer in solid state by single ray diffraction analysis. Resolution of enantiomers in solution by means of chromatographic method using β-cyclodextrin modified stationary phase was also reported for such bridged compounds [24]. This actually exclude the idea that the reason for the symmetric ^{11}B spectral pattern is a racemization due to fast tautomerism in solution of the antiprismatic enantiomers around the unfavorable eclipsed prismatic conformation. Most probably, the small magnitude of the chiral effect and the broadness of the signals are explanations. Also the accidental overlapping of signals can not be excluded. An indication about the asymmetry of the compound **HNEt$_3$[3]** can be found in its ^{1}H NMR spectrum, in which two sets of CH_{carb} resonances at 3.73 and 3.71 ppm, integrated for 2 each, can be seen. Differently, ^{1}H NMR spectrum of **HNEt$_3$[2]** consists of one CH resonance of intensity 4 but two different resonances can be found in its ^{13}C NMR spectrum at 47.87 and 47.75 ppm respectively, which are attributed to cluster carbon atoms. The rest of the peaks in the spectra of both derivatives correspond to the presence of aryl substituent and triethylammonium counter-ion. ^{31}P NMR spectra of both compounds after purification consist of one singlet. The counter-ion is believed to affect directly or indirectly the bridge system, since we observed a shift of the ^{31}P signals of the crude product after treatment with an excess of aqueous solution of $HNEt_3 \cdot HCl$ standardizing the counter-ion. This idea is supported by crystallographic determination of analogous phosphorus bridged chloride [8,8′-μ-O_2POCl-3,3′-Co(1,2-$C_2B_9H_{10})_2]^-$ reported by Plešek and colleagues [23].

As part of our search for possible reasons for the resistance of esters **[2]**$^-$ and **[3]**$^-$ to alkaline hydrolysis, we compared four compounds, the metallacarboranyl-aryl and dialkyl-aryl phosphate triesters (**[3]**$^-$ and paraoxon) and their phosphorothioate counterparts (**[2]**$^-$ and parathion) (Fig. 1).

The hydrolytic process was followed spectrophotometrically by measuring the rate of the release of the 4-nitrophenolate ion in aqueous NaOH solution containing 25% ethanol. Second-order rate constants (K values) were obtained by plotting the pseudo-first order constants (k_{obs}) against the NaOH concentration. The complete set of plots and second-order rate constants are shown in Fig. S14 and Table S1 in the Supporting Information. The susceptibility to hydrolysis was found to decrease in the following order: paraoxon > parathion ≫ **[3]**$^-$ > **[2]**$^-$, with a difference in the rate constants of the alkyl- and metallacarboranyl derivatives of up to four orders of magnitude. The hydrolysis of **[3]**$^-$ with 2 M NaOH at 50 °C is almost complete after 42 h, while only ~40% of **[2]**$^-$ is converted to **[2a]**$^-$. Paraoxon and parathion are almost completely hydrolyzed within 20 min under the same conditions (Fig. 2).

The activation thermodynamic parameters were calculated from the Eyring plots of all four compounds (Fig. S15), and the calculated values shown in Fig. 3. It has to be acknowledged that even if in the 42 h experiment (Fig. 2) the very different hydrolytic behavior between compound **[2]**$^-$ and **[3]**$^-$ is appreciable, the thermodynamic parameters calculated for hydrolysis of compound **[2]**$^-$ are affected by higher uncertainty compared to other compounds, making hydrolysis of **[2]**$^-$ and **[3]**$^-$ not effectively comparable by considering only those values. The large deviation comes from the very low rate of hydrolysis of compound **[2]**$^-$. Since the experimental approach to find the observed constants involves the initial rate determination, the occurrence of errors in the case of compound **[2]**$^-$ were higher among the replicates.

The activation parameters correlate well with the differences in the hydrolysis rates between the alkyl- and metallacarboranyl compounds, as the value of $\Delta H^{\ddagger}$ nearly doubled. Based on the negative activation entropies, it is possible to conclude that all four compounds are hydrolyzed by an associative mechanism. This is in accordance with what was previously found for paraoxon and

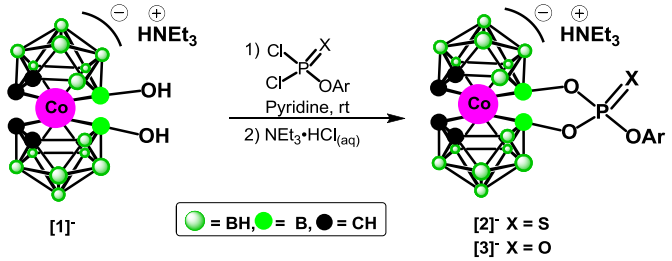

Scheme 1. Synthesis of [8,8′-μ-O_2P(S)$OC_6H_4NO_2$-3,3′-Co(1,2-$C_2B_9H_{10})_2]^-$ **[2]**$^-$ and [8,8′-μ-O_2P(O)$OC_6H_4NO_2$-3,3′-Co(1,2-$C_2B_9H_{10})_2]^-$ **[3]**$^-$. Ar = 4-nitrophenyl.

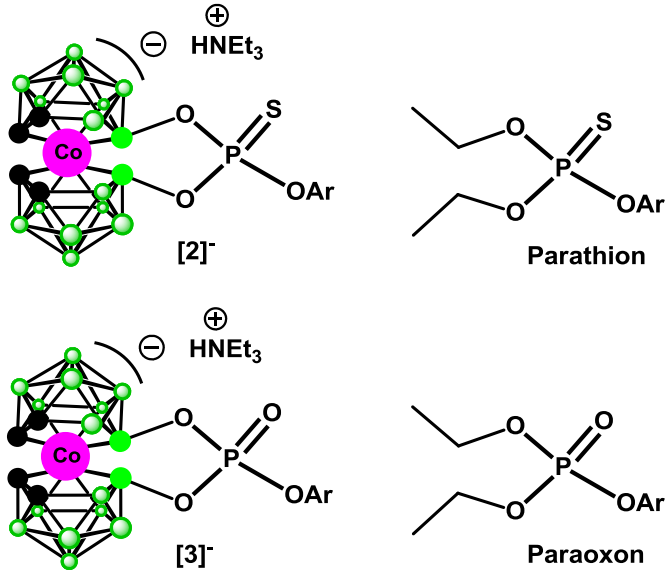

Fig. 1. Metallacarboranyl-aryl and a dialkyl-aryl phosphate triesters and their analogues phosphorothioates used in this study. Ar = 4-nitrophenyl.

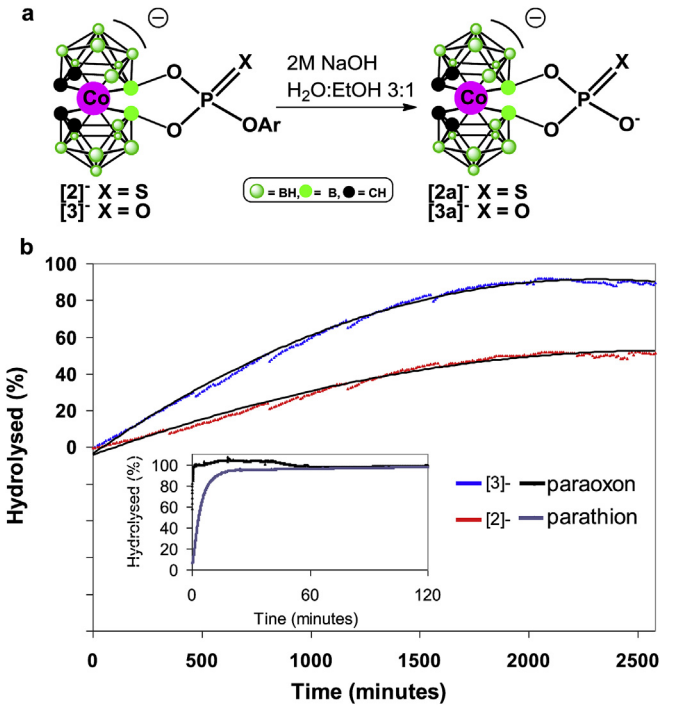

Fig. 2. (a) Alkaline hydrolysis of compounds **[2]**$^-$ and **[3]**$^-$. Hydrolysis was performed in a EtOH/2 M NaOH aq mixture (1:3) at 50 °C. The percentage of hydrolysis [%] *versus* time plots are shown for **[2]**$^-$ and **[3]**$^-$. Paraoxon and parathion are used for comparison (insert). Ar = 4-nitrophenyl.

parathion alkaline hydrolysis [25]. The ratio between the rate constant of the phosphate ester (Ko) and that of its phosphorothioate counterpart (Ks) represents the thio effect (Fig. 3).

The magnitude of the thio effect correlates with the relative timing of the attack of the nucleophile and departure of the living group; hence, it can be a valid tool for elucidating the reaction mechanism and transition state [26,27]. When the reaction proceeds through a transition state in which the P–O bond formation occurs prior to the formation of the bond with the entering nucleophile (dissociative mechanism), the thio substituent is rate enhancing, with ko/ks values lower than 1. This is typical of phosphomonoesters. In the case of phosphotriesters, the thio effect results in a ratio higher than 1 (typically in the 10–160 range) and reflects another scenario in which the nucleophilic attack dominates the reaction coordinate and precedes the P–O (leaving group) bond cleavage (associative mechanism) [26]. As expected, the thio substituent clearly stabilizes the hydrolysis of both the alkyl- and metallacarboranyl analogues of the 4-nitrophenyl phosphate esters analyzed here. In both cases, ko/ks > 1 and $\Delta H^{\ddagger}$ followed a trend compatible with lower reaction rates for the phosphorothioates compared to the phosphate analogues. Although the overall mechanism is the same, the magnitude of the thio effects are very different in these two cases. In the case of paraoxon and parathion, a thio effect of 14.4 at 40 °C was observed, while in the case of bridged metallacarborane esters, the thio effect falls to 2.1 under the same conditions. These data support the hypothesis that in the case of the metallacarborane derivatives, the transition state (TS) (Fig. 3) is less tight, i.e., the participation of the nucleophile is lower, and the transition state is slightly shifted toward the extreme methaphosphate-like TS, which is characteristic of a fully dissociative unimolecular mechanism. This observation fits with the more positive entropy of activation found for metallacarborane derivatives compared to the alkyl derivatives. The importance of $\Delta S^{\ddagger}$ can not be underrated. The contribution of entropy to the different behavior of alkyl- and metallacarboranyl-derivatives can be due to both electrostatic and solvation effects. This is expectable since the studied reaction involves strongly solvated ions. It is indeed not uncommon that reactions involving aqueous hydroxide ion are dominated by entropy because the required desolvation of OH^-. On the other hand, because anionic character of the metallacarborane species an electrostatic shielding of the phosphorus reaction center against approaching nucleophile can be expected to contribute to the entropy factor.

The electron density of the dicarbollide cages is inductively transferred through the more electronegative bridging oxygen atoms, which act as molecular conductors, to the empty d orbitals on the P center, weakening of the electrophilicity of the phosphorus atom. The transfer of the electrons of the nucleophilic agent into these orbitals in the transition state is thus significantly hindered with a concomitant drop in the rate of nucleophilic substitution. Thus, both the shielding effect of the negatively charged metallacarborane towards approaching nucleophile and the inductive effect decreasing the electrophilicity of the phosphorus can combine and contribute to the "metallacarborane effect". It can also be speculated that the formation of the bridge between positions 8

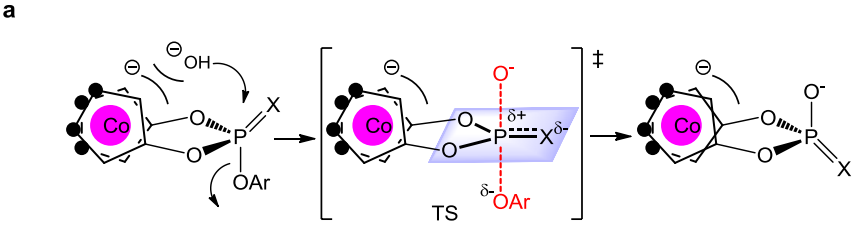

b

	$\Delta G^{\ddagger}$ (kcal mol^{-1})	$\Delta H^{\ddagger}$ (kcal mol^{-1})	$\Delta S^{\ddagger}$ (eu)	Ko/Ks
[2]$^-$	27.02 ± 4.93	23.01 ± 6.23	-12.83 ± 15.75	2.1
[3]$^-$	26.46 ± 0.15	21.12 ± 0.18	-17.08 ± 0.46	
Parathion	22.26 ± 0.42	13.02 ± 0.53	-29.54 ± 1.35	14.4
Paraoxon	20.60 ± 0.08	9.42 ± 0.10	-35.74 ± 0.26	

Fig. 3. (a) Schematic representation of the transition state (TS) in the hydrolysis of metallacarboranyl-aryl esters **[2]**$^-$ and **[3]**$^-$. (b) Activation thermodynamic parameters: metallacarborane and thio effects for the alkaline hydrolysis of $HNEt_3$**[2]**, $HNEt_3$**[3]**, paraoxon and parathion at 40 °C.

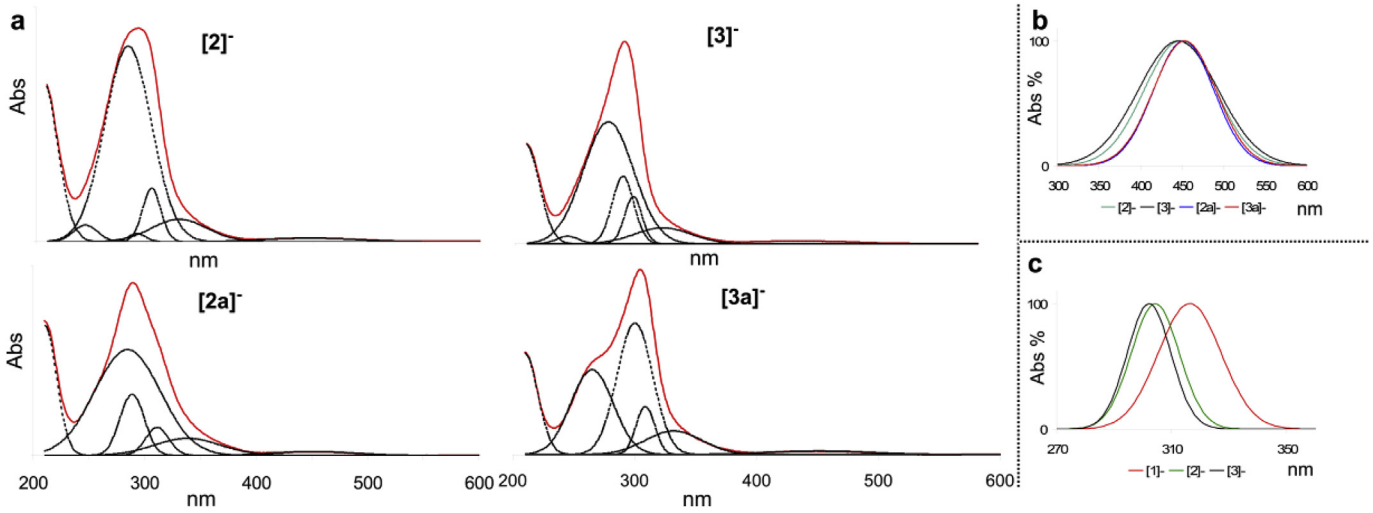

Fig. 4. a) UV–Vis spectra (solid red lines) of compounds **[2]**$^-$, **[2a]**$^-$, **[3]**$^-$, and **[3a]**$^-$ and Gaussians obtained by mean line fitting (dashed black lines). b) Gaussians, obtained from deconvolution, relative to the d-d transition band of compounds **[2]**$^-$, **[2a]**$^-$, **[3]**$^-$, and **[3a]**$^-$. c) Gaussians relative to the band at approximately 320 nm for compounds **[1]**$^-$, **[2]**$^-$ and **[3].** (For interpretation of the references to colour in this figure legend, the reader is referred to the Web version of this article.)

and 8' forces the compound to maintain a conformation with higher polarization because all four $\delta+$ carbon vertices are concentrated on one side of the molecule. In this conformation the inductive transfer of electron density could result more pronounced.

Involment of hyperconjugation has been also considered. In particular it was considered the kinetic consequences stemming from electron density delocalization from the B–O oxygen atom lone pair into the P—$OPhNO_2$ sigma antibonding orbital [28]. This effect would preferentially stabilize a resonance structure double-bond/no bond, which is close to product formed after hydrolysis. Therefore the consequence for the occurrence of hyperconjugation would be the increase in the hydrolysis rate for metallacarboranyl-derivatives compared to those of alkyl derivatives. Since this is not the case, the involvement of such stereoelectronic effect can be excluded.

The electronic interaction between the cluster and the outer phosphorus bridge of the molecule is clearly reflected in the UV–Vis spectroscopic properties. Teixidor and coworkers [29,30] reported the UV/Vis spectrum of [3; 3′-Co(1; 2-$C_2B_9H_{11}$)$_2$]$^-$ in acetonitrile to account for four absorption bands at 207; 281; 337; 445 nm respectively. This is in agreement with what we found by recording and deconvoluting the spectrum of [3; 3′-Co(1; 2-$C_2B_9H_{11}$)$_2$]- in the same solvent. UV–Vis spectra and results of line fitting are reported in Fig. 4 and Table 1.

The d-d transition band at approximately 450 nm, which depends on the electronic environment around the Co center, appears to be bathochromically shifted by 5 and 7 nm in the spectra of **[2a]**$^-$ and **[3a]**$^-$, respectively, i.e., after the leaving of the 4-nitrophenolate ion (Fig. 4b). Second, the absorption at approximately 310 nm appears blueshifted for **[2]**$^-$ and **[3]**$^-$ compared to bis-hydroxy precursor **[1]**$^-$ (Fig. 4c). This band, which is absent in the spectrum of [3,3′-Co(1,2-$C_2B_9H_{11}$)$_2$]$^-$, has been attributed to atoms bearing unshared n electrons or π systems directly bound at position 8 of the dicarbollide moiety in the metallacarboranes [30]. The shift to a higher wavelength is due to the conjugation of the cluster with the phosphorus 3d orbitals. The full set of numeric values for the UV absorption maxima of compounds **[1]**$^-$, **[2]**$^-$, **[2a]**$^-$, **[3]**$^-$, **[3a]**$^-$ and [3,3′-Co(1,2-$C_2B_9H_{11}$)$_2$] are provided in Table 1.

In accordance with the rules of nucleophilic substitution at a tetrahedral phosphorus atom, the most likely structure of the transition state is a trigonal bipyramid in which the entering and leaving groups occupy the axial positions. The bulky, negatively charged Co bis(dicarbollide) part, positioned to allow the O–P–O group to occupy an equatorial position, could represent both an electrostatic and steric barrier that slows the nucleophilic attack. Moreover, the rearrangement of the substituents around the phosphorus center during the formation of the transition state requires a change in the O–P–O (with an angle equal to 120°) and B–O–P angles, as represented in Fig. 3.

We hypothesize that the steric hindrance and limited flexibility of the bridge required for the rearrangement in the transition state are also factors that contribute to the amazing stability of these compounds. Alkoxy cyclic phosphate ester **4** (Fig. 5) has been found to hydrolyze much more easily than the metallacarboranyl phosphate triester even when the same leaving group and the same number of atoms are present in the bridge and in the ring.

This 6-membered bridge behaved similarly to the acyclic paraoxon (second-order rate constant for the hydrolysis of 2-aryloxy-2-oxo-1,3,2-dioxaphosphorinan [31] with NaOH at 39 °C $= 7.5 \cdot 10^{-2}\ M^{-1}\ s^{-1}$). In general, six-membered cyclic triesters react at rates that are comparable to those of acyclic triesters [32,33].

Table 1
UV–Vis spectra of compounds [1]$^-$, [2]$^-$, [2a]$^-$, [3]$^-$, [3a]$^-$ in acetonitrile.

Compound	λ (nm)[a]						
[3,3′-Co(1,2-$C_2B_9H_{11}$)$_2$]	211			281		329	449
[1]$^-$	213		265	300	316	341	453
[2]$^-$	206	245	283	291	304	329	447
[2a]$^-$	210		285	289	311	339	452
[3]$^-$	209	245	281	293	302	328	445
[3a]$^-$	210		264	298	308	290	452

[a] Values obtained after line fitting analysis.

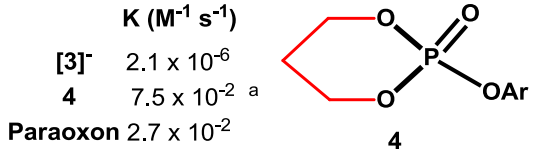

Fig. 5. Comparison between second order hydrolysis constant (K) of 2-aryloxy-2-oxo-1,3,2-dioxaphosphorinan **4** (39 °C [31]), $HNEt_3$**[3]**, and paraoxon at 40 °C.

3. Conclusion

In summary, it was shown that, compared to the alkoxy group, metallacarboranes reduce the reactivity of the phosphorus bridged metallacarborane esters by weakening the electrophilicity of the associated phosphorus atom due to the inductive effect of the cluster as well as the electrostatic shielding of the phosphorus center by the metallacarborane, hindering the approach of the negatively charged nucleophile. These effects in addition to the steric hindrance and limited flexibility of the atypical six-membered ring formed by the phosphorus, oxygens, boron atoms and cobalt, can overall be called the "metallacarborane effect". They are the major factors influencing the reactivity of the phosphate and phosphorothioate functional groups bonded through a bridge, while the thio effect plays a minor role in this case. Thus, our findings clearly indicate that a metallacarborane cannot be considered a "spectator" nonleaving group, and instead, it plays a very significant role as a deactivator of the reaction at the reactive phosphate and phosphorothioate triesters, directly affecting the stability of the transition state and hence its hydrolytic susceptibility. This observation is in accordance with the slow (though much faster than for **[3]**$^-$) hydrolysis of chloride salt [3,3′-Co-8,8′-μ-$O_2P(O)Cl(1,2\text{-}C_2B_9H_{10})_2]^-$ reported earlier by Grüner et al. [23]. Finally, these systems could be valid models to study nonleaving group effects [34,35] on the reactivity of phosphate and phosphorothioate triesters and to explore new approaches for the chemical manipulation of metallacarboranes. This would significantly broaden the applicability of metallacarboranes not only in catalysis but also in a number of other potential applications.

4. Experimental section

4.1. Materials

All solvents were purchased in the highest available quality required for the specific application. Where required, reactions were performed under argon atmosphere using anhydrous solvents treated with heat activated molecular sieves for at least 24 h. Operations such as chromatography and crystallization, were carried out in the air. Molecular sieves (4 Å and 3 Å) were purchased by Alfa Aesar. Triethylamine, pyridine anhydrous, 4-nitrophenyl phosphorodichloridate, P_2O_5, sodium hydroxide, O,O-diethyl O-(4-nitrophenyl) phosphorothioate (parathion) and O,O-diethyl O-(4-nitrophenyl) phosphate (paraoxon) were purchased from Sigma Aldrich. Cobalt bis(1,2-dicarbollide) was purchased from Katchem Ltd., Czech Republic. 8,8′-dihydroxy derivative of cobalt bis(1,2-dicarbollide) **$HNEt_3$[1]** was synthesized according to the procedure reported by Plešek et al. [36] Spectroscopic properties are in agreement with those previously reported (data not shown).

4.2. Chromatography

Analytical HPLC to check purity of products was performed on a DIONEX Ultramate 3000 HPLC system equipped with a photodiode array detector (fixed wavelengths 268, 280, 295, 309, 458 nm). The method consisted in a gradient elution from 20% to 60% aqueous acetonitrile trough a Thermo Scientific Hypersil Gold (5 μm particle size) reverse phase column at 25 °C. HPLC data were acquired and processed by Chromaleon 6.8 software. Chromatography for purification of products was performed on a 230–400 mesh silica gel (Sigma Aldrich) filled glass column. TLC was performed on F254 silica gel on Al foils purchased by Sigma Aldrich. Compounds were visualized using UV light (254 nm) and by staining with 0.05 %w/v palladium chloride solution in MeOH/HCl.

4.3. NMR

^1H, ^{11}B, ^{13}C and ^{31}P NMR spectra were recorded in acetonitrile-d_3 with a Bruker Advance III 600 MHz spectrometer. Residual solvent resonances were taken as references in ^{13}C (CD_3CN: 118.26 ppm) and ^1H NMR (CD_3CN: 1.94 ppm) spectra.

4.4. FT-IR spectroscopy

Infrared absorption spectra were recorded using a Nicolet 6700 FT-IR spectrometer (Thermo Scientific) equipped with a Smart orbit diamond Attenuated Total Reflectance (ATR) accessory. Samples to be analyzed were placed on a diamond ATR element in the solid form or by casting from CH_2Cl_2 solution. Data were acquired and processed by Omnic 8.1 software.

4.5. UV/Vis spectrometry and deconvolution of spectra

UV/Vis absorption spectra (190–600 nm) were recorded with a Jasco V-750 spectrophotometer at 25 °C in acetonitrile; by using QS high precision cell with 1 cm light path. Molar extinction coefficients (ε; L mol^{-1} cm^{-1}) of were determined according to Lambert-Beer law as the slope of linear fitting curve of absorbance versus concentration plots (Fig. S13). ε equal to 33164 and 43640 L mol^{-1} cm^{-1} were found for **$HNEt_3$[2]** and **$HNEt_3$[3]** respectively. To resolve complex spectra into individual bands with defined absorption maxima; a line fitting analysis was performed for each compound. The curves composing the spectra were simulated with a Gaussian distribution assuming the cumulative spectra is the mathematical sum of the various distributions and assuming a linear correlation between raw data and the simulated distributions. The good of fitting (R^2) for all the spectra deconvolution was 0.9999 with fitting error in the range 0.08250–0.00074. Therefore; relevant comparison was guaranteed.

Hydrolytic studies. Alkaline hydrolysis reactions were followed recording the absorbance due to p-nitrophenolate production; at 400 nm in a Jasco V-750 UV-spectrophotometer equipped with a temperature controller and a peltier thermostated cell holder. Stock solutions of parathion ($4.17\cdot10^{-4}$ M); paraoxon ($4.44\cdot10^{-4}$ M); **$HNEt_3$[2]** ($5.11\cdot10^{-4}$ M) or **$HNEt_3$[3]** ($6.05\cdot10^{-4}$ M) in ethanol were prepared and aliquots of these (0.5 ml) were added to 1.5 ml of aqueous sodium hydroxide to initiate hydrolysis. Reactions were followed for 1 h and rate constants were obtained from the initial rates method under pseudo-first order conditions ([NaOH]/[substrate]>100). Five hydroxide final concentrations (in the range 0.02–1.00 M) were used in order to determine second order rate constants; and the reaction were repeated at five different temperatures (in the range 35–60 °C). Activation parameters were calculated from Eyring plots; using second-order rate constants.

Reaction of parathion; paraoxon; **$HNEt_3$[2]** or **$HNEt_3$[3]** were also followed spectrophotometrically to completeness by recording the full spectra from 190 to 600 nm; one every 10 min. In this case; a final concentration of substrate of $2.78\cdot10^{-5}$ M) and 2 M NaOH in water: ethanol 3 : 1 bv and a temperature of 50 °C were applied.

4.6. Synthesis of [8,8′-μ-$O_2P(S)OC_6H_4NO_2$-3,3′-$Co(1,2\text{-}C_2B_9H_{10})_2]^-$ $HNEt_3$ [2]

To a stirred solution of **$HNEt_3$[1]** (200 mg, $43.7\cdot10^{-2}$ mmol) in anhydrous pyridine (2.2 ml) a solution of *p*-nitrophenyl dichlorothiophosphonate (119 mg, $43.7\cdot10^{-2}$ mmol) in the same solvent (2.2 ml) was added dropwise. The mixture was stirred for 18 h at ambient temperature. Then, the reaction was quenched with water (8 ml). Chloroform (1 mL) was added and the organic layer was separated. The aqueous layer was extracted with chloroform

(3 × 7 mL). The combined organic phase was washed with water (3 × 1 ml) and dried over anhydrous $MgSO_4$ prior to evaporation to dryness under reduced pressure. The residue was dissolved in the minimum volume of ethanol and an aqueous solution containing an excess of $NEt_3 \cdot HCl$ was added, resulting in the formation of a precipitate. This was filtered, washed with water and dried under vacuum. The resulting solid was dissolved in CH_2Cl_2 and purified by silica gel column chromatography by a gradient elution (0–20% of CH_3CN in $CHCl_3$). Fraction containing the product were collected together and the solvent evaporated to dryness, affording 182 mg of an orange solid. Yield 75%. Purity 99.07% (HPLC). TLC (CH_3CN:$CHCl_3$ 1:2) Rf 0.61. UV–Vis (CH_3CN) λ_{max} (nm) 293, 446.

HPLC k' 4.26. MS (FAB): *m/z*: calcd (100%): 554.85 $[M]^-$; found: 555.4 (100%). ^1H NMR (500 MHz, CD_3CN, ppm) δ 8.21 (d, $J = 9.1$ Hz, 2H, arom. CH_{metha}), 7.38 (d, $J = 9.0$ Hz, 2H, arom. CH_{ortho}), 3.71 (s, 4H, CH_{carb}), 3.13 (q, $J = 7.3$ Hz, 6H, $HN(CH_2CH_3)_3$), 1.23 (t, $J = 7.3$ Hz, 9H, $HN(CH_2CH_3)_3$). $^{13}C\{^1H\}$ NMR (126 MHz, CD_3CN, ppm) δ 157.5 (arom. OC), 145.2 (arom. C_{para}), 126.1 (arom. C_{metha}), 122.4 (arom. C_{ortho}), 47.9 ($HN(\underline{CH_2}CH_3)_3$), 47.8 ($CH_{carb}$), 47.7 ($CH_{carb}$), 9.1 ($HN(CH_2\underline{CH_3})_3$). $^{11}B\{^1H\}$ NMR (160 MHz, CD_3CN, ppm) δ 23.0 (s, 2B), −2.6 (s, 2B), −5.6 (s, 4B), −8.4 (s, 4B), −18.8 (s, 4B), −27.7. (s, 2B). $^{31}P\{^1H\}$NMR (243 MHz, CD_3CN, ppm): δ 49.0. FT-IR ATR (cm^{-1}): 3647; 3038; 2988; 2547 (ν B–H); 1610, 1590 (δ out of plane = C–H aromatic); 1519 (ν C=C); 1489 (ν asym NO_2); 1471; 1456; 1392; 1342 (ν sym NO_2); 1290; 1237; 1127; 1093; 1013; 981; 950 (ν P–O); 900; 877; 859; 788; 760 (ν P=S); 747; 689; 661.

4.7. Synthesis of [8; 8′-μ-$O_2P(O)OC_6H_4NO_2$-3; 3′-Co(1; 2-$C_2B_9H_{10})_2]^-$ $HNEt_3$ [3]

$HNEt_3$[1] (60 mg; $13.1 \cdot 10^{-2}$ mmol) was dissolved in anhydrous pyridine (0.5 ml). A solution of 4-nitrophenyl phosphorodichloridate (33.5 mg; $13.1 \cdot 10^{-2}$ mmol) in the same solvent (0.5 ml) was added dropwise. The mixture was stirred for 3h at ambient temperature. Then; the reaction was quenched with water (3 mL) and extracted with chloroform (3 × 7 mL). The combined organic phase was washed with water (3 × 1 ml) and dried over anhydrous $MgSO_4$ prior to evaporation to dryness under reduced pressure. The residue was dissolved in the minimum volume of ethanol and an aqueous solution containing an excess of $NEt_3 \cdot HCl$ was added; resulting in the formation of a precipitate. This was filtered; washed with water ad dried under vacuum. The resulting solid was dissolved in CH_2Cl_2 and purified by silica gel column chromatography by a gradient elution (0–20% of CH_3CN in $CHCl_3$). Fraction containing the product were collected together and the solvent evaporated to dryness; affording 78 mg of an orange solid. Yield 93%. Purity 98.99% (HPLC). TLC (CH_3CN:$CHCl_3$ 1:2) Rf 0.58. HPLC k' 4.43. UV–Vis (CH_3CN) λ_{max} (nm) 295, 452.MS (ESI): *m/z*: calc (100%) 539.246 $[M]^-$; found: 539 (100%). ^1H NMR (600 MHz; CD_3CN; ppm) δ 8.22 (d; $J = 9.1$ Hz; 2H; 2H; arom. CH_{metha}); 7.38 (d; $J = 8.7$ Hz; 2H; arom. CH_{ortho}); 3.73 (s; 2H; CH_{carb}); 3.71 (s; 2H; CH_{carb}); 3.07 (q; $J = 7.3$ Hz; 6H; $HN(\underline{CH_2}CH_3)_3$); 2.23 (s; 9H; $HN(CH_2\underline{CH_3})_3$); 1.20 (t; $J = 7.3$ Hz; 9H). $^{13}C\{^1H\}$ NMR (151 MHz; CD3CN) δ 157.4 (d; $J = 4.8$ Hz; arom. OC); 145.1 (s; arom. C_{para}); 126.4 (s; arom. C_{metha}); 121.6 (d; $J = 5.7$ Hz; arom. C_{ortho}); 47.9 (s; $HN(\underline{CH_2}CH_3)_3$); 47.7 (s; CH_{carb}); 9.1 (s; $HN(CH_2\underline{CH_3})_3$). ^{11}B NMR (193 MHz; CD_3CN; ppm) δ 23.4 (s; 2B); −2.7 (s; 2B); −5.7 (s; 4B); −8.4 (s; 4B); −18.8 (s; 4B); −27.8 (s; 2B). ^{11}B NMR (193 MHz; CD_3CN; ppm) δ 23.4 (s; 2B); −2.7 (d; $J = 141.0$ Hz; 2B); −5.7 (d; $J = 138.1$ Hz; 4B); −8.4 (d; $J = 139.0$ Hz; 4B); −18.8 (d; $J = 152.0$ Hz; 4B); −27.9 (d; $J = 134.5$ Hz; 2B). $^{31}P\{^1H\}$NMR (202 MHz; CD_3CN; ppm): δ −14.9. FT-IR ATR (cm^{-1}): 3648; 3038; 2996; 2700; 2547 (ν B–H); 1612, 1591 (δ out of plane = C–H aromatic); 1519 (ν C=C); 1490 (ν asym NO_2); 1473; 1448; 1394; 1344 (ν sym NO_2); 1292; 1231 (ν P=O); 1133; 1104; 1004; 981; 951 (ν P–O); 932; 901; 874; 859; 846 (=C–H); 788; 744; 689; 667.

4.8. Statistical analysis

Uncertainty for the fitted values was estimated after least square procedure by LINEST function on Microsoft Excel software.

Acknowledgements

This research was financially supported by The National Science Centre in Poland, Grant number 2015/16/W/ST5/00413 for years 2015–2021. A contribution from the Statutory Fund of IMB PAS is also gratefully acknowledged.

Appendix A. Supplementary data

Supplementary data to this article can be found online at https://doi.org/10.1016/j.jorganchem.2019.06.001.

References

[1] Organometallic chemistry of boranes and carboranes (to be dedicated to professor Narayan Hosmane), in: R. Adams, V.I. Bregadze (Eds.), Special Issue in Journal of Organometallic Chemistry, vol. 865, Elsevier B.V., 2018. https://www.sciencedirect.com/journal/journal-of-organometallic-chemistry/vol/865/suppl/C.

[2] Organometallic chemistry of polyhedral boranes and carboranes: synthesis, theory, and application, in: N.S. Hosmane, S.R. Adams (Eds.), Special Issue in Journal of Organometallic Chemistry, vol. 798, Elsevier B.V., 2015. Part 1, https://www.sciencedirect.com/journal/journal-of-organometallic-chemistry/vol/798/part/P1.

[3] N.S. Hosmane, R. Eagling, Handbook of Boron Science, WORLD SCIENTIFIC (EUROPE), 2018, https://doi.org/10.1142/q0130-vol4.

[4] R.N. Grimes, Metallacarboranes in the new millennium, Coord. Chem. Rev. 200–202 (2000) 773–811, https://doi.org/10.1016/S0010-8545(00)00262-9.

[5] B.P. Dash, R. Satapathy, B.R. Swain, C.S. Mahanta, B.B. Jena, N.S. Hosmane, Cobalt bis(dicarbollide) anion and its derivatives, J. Organomet. Chem. (2017) 849–850, https://doi.org/10.1016/j.jorganchem.2017.04.006, 170–194.

[6] I.B. Sivaev, V.I. Bregadze, Chemistry of cobalt bis(dicarbollides). A review, Collect. Czechoslov. Chem. Commun. 64 (2002) 783–805, https://doi.org/10.1135/cccc19990783.

[7] D.M.P. Mingos, R.H. Crabtree (Eds.), Comprehensive Organometallic Chemistry III, Elsevier, 2007. https://www.sciencedirect.com/referencework/9780080450476/comprehensive-organometallic-chemistry-iii#book-description. (Accessed 10 May 2019).

[8] M.F. Hawthorne, D.C. Young, P.A. Wegner, Carbametallic boron hydride derivatives. I. Apparent analogs of ferrocene and ferricinium ion, J. Am. Chem. Soc. 87 (1965) 1818–1819, https://doi.org/10.1021/ja01086a053.

[9] G.M.A. Junqueira, Remarkable aromaticity of cobalt bis(dicarbollide) derivatives: a NICS study, Theor. Chem. Acc. 137 (2018) 92, https://doi.org/10.1007/s00214-018-2272-6.

[10] P. Farràs, E.J. Juárez-Pérez, M. Lepšík, R. Luque, R. Núñez, F. Teixidor, Metallacarboranes and their interactions: theoretical insights and their applicability, Chem. Soc. Rev. 41 (2012) 3445, https://doi.org/10.1039/c2cs15338f.

[11] V.N. Romanovskiy, I.V. Smirnov, V.A. Babain, A. Yu Shadrin, Combined processes for high level radioactive waste separations: UNEX and other extraction processes, in: Adv. Sep. Tech. Nucl. Fuel Reprocess. Radioact. Waste Treat, Woodhead Publishing, 2011, pp. 229–265, https://doi.org/10.1533/9780857092274.2.229.

[12] B. Grüner, J. Rais, P. Selucký, M. Bubeníková, Recent progress in extraction agents based on cobalt bis(dicarbollides) for partitioning of radionuclides from high-level nuclear waste, in: S. Hosmane (Ed.), Boron Sci. New Technol. Appl. N, CRC Press, Boca Raton, 2012, pp. 463–490, https://doi.org/10.1201/b11199.

[13] Z.J. Leśnikowski, Challenges and opportunities for the application of boron clusters in drug design, J. Med. Chem. 59 (2016) 7738–7758, https://doi.org/10.1021/acs.jmedchem.5b01932.

[14] W.J. DuBay, P.A. Grieco, L.J. Todd, Lithium cobalt-bis-dicarbollide: a novel Lewis acid catalyst for the conjugate addition of silyl ketene acetals to hindered .alpha.,.beta.-Unsaturated carbonyl compounds, J. Org. Chem. 59 (1994) 6898–6899, https://doi.org/10.1021/jo00102a009.

[15] P.A. Grieco, W.J. DuBay, L.J. Todd, Lithium cobalt-bis-dicarbollide catalyzed substitution reactions of allylic acetates, Tetrahedron Lett. 37 (1996) 8707–8710, https://doi.org/10.1016/S0040-4039(96)02021-7.

[16] T. Akiyama, K. Saito, S. Janczak, Z. Lesnikowski, Phosphoric acid bridged cobalt bis(dicarbollide) ion as a highly efficient catalyst for the organocatalytic hydrogenation of ketimines, Synlett 25 (2014) 795–798, https://doi.org/10.1055/s-0033-1340847.

[17] J. Plešek, I. Císařová, J. Bačkovský, Cobalt bis(1,2-dicarbollide) ion with a disulfur bridge between B(8) and B(8′). X-ray structure, absolute configuration of one enantiomer, and implications, Collect. Czechoslov. Chem. Commun. 67 (2002) 569–576, https://doi.org/10.1135/cccc20020569.
[18] J. Plesek, B. Gruner, J. Holub, Synthesis and properties of cobaltacarboranes with substituted monoatomic bridges between ligands of the 6,6'-mu-RnE(1,7-C2B9H10)(2)-2-Co type, Collect. Czechoslov. Chem. Commun. 62 (1997) 884–893, https://doi.org/10.1135/cccc19970884.
[19] J. Plesek, S. Hermanek, K. Base, L.J. Todd, W.F. Wright, Zwitterionic compounds of 8,8'-X(C2b9h10)2co series with monoatomic O, S, Se, Te, N bridges between carborane ligands, Collect. Czechoslov. Chem. Commun. 41 (1976) 3509–3515, https://doi.org/10.1135/cccc19763509.
[20] B. Grüner, I. Cisařová, A. Franken, J. Plešek, Resolution of the [6,6'-μ-(CH3)2P-(1,7-(C2B9H10)2)-2-Co] bridged cobaltacarborane to enantiomers pure by chiral HPLC, circular dichroism spectra and absolute configurations by X-ray diffraction, Tetrahedron Asymmetry 9 (1998) 79–88, https://doi.org/10.1016/S0957-4166(97)00605-8.
[21] A. Franken, J. Plešek, J. Fusek, M. Semrau, Cobaltacarboranes with intramolecular monophosphorus bridges 8,8'-μ-Me2P(1,2-C2B9H10)2-3-Co, 6,6'-μ-Me2P(1,7-C2B9H10)2-2-Co and the respective non-bridged trimethylphosphine derivatives (8-me3P-1,2-C2B9H10)-3-Co-(1,2-C2B9H11) and (6-me3P-1,7-C2B9H10)-2-Co, Collect. Czechoslov. Chem. Commun. 62 (1997) 1070–1079, https://doi.org/10.1135/cccc19971070.
[22] Z. Janoušek, J. Plešek, S. Heřmánek, K. Baše, L.J. Todd, W.F. Wright, Synthesis and characteristics of sulfur interligand bridge-derivatives and of some S-substituted compounds in the (C2B9H11)2Co- series. Conformations of (C2B9H11)2Mx- metallocarboranes, Collect. Czechoslov. Chem. Commun. 46 (1981) 2818–2833, https://doi.org/10.1135/cccc19812818.
[23] J. Plešek, B. Grüner, I. Císařová, J. Báča, P. Selucký, J. Rais, Functionalized cobalt bis(dicarbollide) ions as selective extraction reagents for removal of M2+ and M3+ cations from nuclear waste, crystal and molecular structures of the [8,8′-μ-ClP(O)(O)2(1,2-C2B9H10)2-3,3′-Co]HN(C2H5)3 and [8,8′-μ-Et2NP(O)(O)2(1,2-C2B9H10)2-3,3′-Co](HN(CH3)3), J. Organomet. Chem. 657 (2002) 59–70, https://doi.org/10.1016/S0022-328X(02)01325-6.
[24] J. Plešek, B. Grüner, J. Fusek, H. Votavová, Asymmetric cobaltacarboranes [6,6'-μ-R-S(1,7-C2B9H10)2-2-Co] with a monosulfur bridge between ligands and HPLC resolution of the enantiomers, Collect. Czechoslov. Chem. Commun. 58 (1993) 2936–2943, https://doi.org/10.1135/cccc19932936.
[25] J. Purcell, A.C. Hengge, The thermodynamics of phosphate versus phosphorothioate ester hydrolysis, J. Org. Chem. 70 (2005) 8437–8442, https://doi.org/10.1021/jo0511997.
[26] A.T.P. Carvalho, A.C. O'Donoghue, D.R.W. Hodgson, S.C.L. Kamerlin, Understanding thio-effects in simple phosphoryl systems: role of solvent effects and nucleophile charge, Org. Biomol. Chem. 13 (2015) 5391–5398, https://doi.org/10.1039/C5OB00309A.
[27] M. Ora, T. Lönnberg, H. Lönnberg, Thio effects as a tool for mechanistic studies of the cleavage of RNA phosphodiester bonds: the chemical basis, in: From Nucleic Acids Seq. To Mol. Med, Springer Berlin Heidelberg, Berlin, Heidelberg, 2012, pp. 47–65, https://doi.org/10.1007/978-3-642-27426-8_3.
[28] E.A. Ruben, J.A. Plumley, M.S. Chapman, J.D. Evanseck, Anomeric effect in "high energy" phosphate bonds. Selective destabilization of the scissile bond and modulation of the exothermicity of hydrolysis, J. Am. Chem. Soc. 130 (2008) 3349–3358, https://doi.org/10.1021/ja073652x.
[29] P. Farràs, F. Teixidor, I. Rojo, R. Kivekäs, R. Sillanpää, P. González-Cardoso, C. Viñas, Relaxed but highly compact diansa metallacyclophanes, J. Am. Chem. Soc. 133 (2011) 16537–16552, https://doi.org/10.1021/ja205850p.
[30] I. Rojo, F. Teixidor, C. Viñas, R. Kivekäs, R. Sillanpää, Relevance of the electronegativity of boron inη5-coordinating ligands: regioselective monoalkylation and monoarylation in cobaltabisdicarbollide[3,3′-Co(1,2-C2B9H11)2]− clusters, Chem. Eur J. 9 (2003) 4311–4323, https://doi.org/10.1002/chem.200304970.
[31] S.A. Khan, A.J. Kirby, The reactivity of phosphate esters. Multiple structure-reactivity correlations for the reactions of triesters with nucleophiles, J. Chem. Soc. B Phys. Org. 0 (1970) 1172–1182, https://doi.org/10.1039/J29700001172.
[32] W.S. Wadsworth, Y.G. Tsay, Nucleophilic substitution at phosphorus. Phosphorothioates, J. Org. Chem. 39 (1974) 984–989, https://doi.org/10.1021/jo00921a027.
[33] W.W. Cleland, A.C. Hengge, Enzymatic mechanisms of phosphate and sulfate transfer, Chem. Rev. 106 (2006) 3252–3278, https://doi.org/10.1021/cr050287o.
[34] A.J. Kirby, M. Medeiros, P.S.M. Oliveira, E.S. Orth, T.A.S. Brandão, E.H. Wanderlind, A. Amer, N.H. Williams, F. Nome, Activating water: important effects of non-leaving groups on the hydrolysis of phosphate triesters, Chem. Eur J. 17 (2011) 14996–15004, https://doi.org/10.1002/chem.201101926.
[35] A.J. Kirby, J.R. Mora, F. Nome, New light on phosphate transfer from triesters, Biochim. Biophys. Acta Protein Proteonomics 1834 (2013) 454–463, https://doi.org/10.1016/j.bbapap.2012.04.010.
[36] J. Plešek, B. Grüner, J. Báča, J. Fusek, I. Císařová, Syntheses of the B(8)-hydroxy- and B(8,8′)-dihydroxy-derivatives of the bis(1,2-dicarbollido)-3-cobalt(1-)ate ion by its reductive acetoxylation and hydroxylation: molecular structure of [8,8′-μ-CH3C(O)2(1,2-C2B9H10)2-3-Co]0 zwitterion determined by X-ray diffraction analysis, J. Organomet. Chem. 649 (2002) 181–190, https://doi.org/10.1016/S0022-328X(02)01115-4.